Effects of impurities on one-dimensional migration of interstitial clusters in iron under electron irradiation

Y. Satoh, H. Matsui, and T. Hamaoka

Institute for Materials Research, Tohoku University, 2-1-1 Katahira, Aoba-ku, Sendai 980-8577, Japan

One-dimensional (1D) migration of small interstitial-type dislocation loops was studied for Fe specimens of different purities at room temperature under electron irradiation using a high-voltage electron microscope. Most 1D migration appeared as discrete jumps (stepwise positional changes) at irregular intervals, and sometimes involved back and forth motion between certain points. The distribution of jump distances extended to over 100 nm in high-purity specimens; it was less than 30 nm in low-purity specimens. Jump frequency was almost proportional to electron beam intensity and was on the same order as the rate of atomic displacement by electron irradiation. Molecular dynamics simulation suggested the suppression of 1D migration of an interstitial cluster (7i) by an oversized solute Cu atom located in the dilatational strain field of the cluster. We proposed that the 1D jump process occurs in the following sequence: (1) interstitial clusters are in a stationary state due to trapping effect by impurity atoms, (2) incident electrons hit and displace impurity atom to cause detrapping, (3) liberated clusters cause fast 1D migration at low activation energy, and (4) the cluster is trapped again by another impurity. Experimental results were analyzed and discussed in terms of the proposed model.

PACS number(s): 61.72.J−, 61.80.Fe, 66.30.Lw

I. INTRODUCTION

Molecular dynamics (MD) simulations of displacement collision cascades in copper and iron have suggested that interstitial clusters are directly formed from cascade damage.[1–3] These small interstitial clusters are considered to escape from the cascade damage zone through one-dimensional (1D) migration because the activation energy for the 1D migration of small interstitial clusters has been suggested to be as low as $0.03–0.05$ eV.[4–8] Migration of single vacancies, on the other hand, is through a three-dimensional random walk. The difference in the migration mechanism between interstitial atoms (including their clusters) and vacancies has been shown to affect total defect structural development under irradiation with high-energy particles.[9–12] Therefore, the study of 1D migration is important for the lifetime prediction and evaluation of light water reactor component materials and for materials development for future nuclear applications. In addition, recent years have seen a renewal of interest in the nature of self-interstitial atoms and their clusters: the 1D migration observed in experiments and MD simulations raises a question about our understanding of the configuration and migration of this basic unit of crystal lattice defects in both fcc and bcc metals.

There are only a few experimental methods for directly detecting the 1D migration of interstitial clusters. Kiritani[13,14] pointed out that a quick back and forth motion of interstitial clusters observed with transmission electron microscopy (TEM) is the 1D migration of "crowdion bundles." The 1D migration behavior of interstitial clusters has been reported for pure metals and alloys under electron irradiation,[15,16] ion irradiation,[17] and annealing after electron irradiation;[16,18] in addition, vacancy-type dislocation loops have been reported to cause the 1D migration.[19] The 1D migration of interstitial clusters was mainly along the directions of the close packing orientation of atoms, namely, $\langle 110 \rangle$ in fcc and $\langle 111 \rangle$ in bcc, which is consistent with the results of

MD simulations. However, there is an apparent discrepancy: experimental 1D migration has been observed as intermittent 1D jumps at room temperature, while MD simulation predicts a fast and continuous 1D random walk even at low temperatures because of the low activation energy for 1D migration.

In this study, we investigated the experimental 1D migration of interstitial clusters in iron specimens of different purities under electron irradiation. We found that some impurity atoms have strong effects on experimental 1D migration behavior. We also performed simple model calculations of the interactions between a small interstitial cluster (7i) and a solute copper atom to support the interpretation of the experimental results. We then proposed a mechanism for the 1D jump behavior observed under electron irradiation by taking the effects of impurities into account. The model interprets the discrepancy in 1D migration behavior between the experiments and MD simulations, as well as the physical significance of the frequency and distance of experimental 1D jumps. The present results and the proposed model offer a key to understanding the intrinsic properties and processes of 1D migration of interstitial clusters under conditions without irradiation.

II. EXPERIMENTAL PROCEDURE

Five iron specimens, which are denoted as Fe1–Fe5, were used. Fe2, Fe3, Fe4, and Fe5 were commercially obtained. The chemical compositions of these specimens were determined. The amounts of carbon and oxygen were determined by the infrared absorption method, and those of hydrogen and nitrogen by the thermal conductivity method. The other elements shown in Fig. 1 were analyzed by glow discharge mass spectrometry (GDMS). In Fig. 1, the white bars show the lower detection limits and the shaded bars on the white bars show the value determined in the analysis. If we exclude the elements below the detection limit, the total amounts of
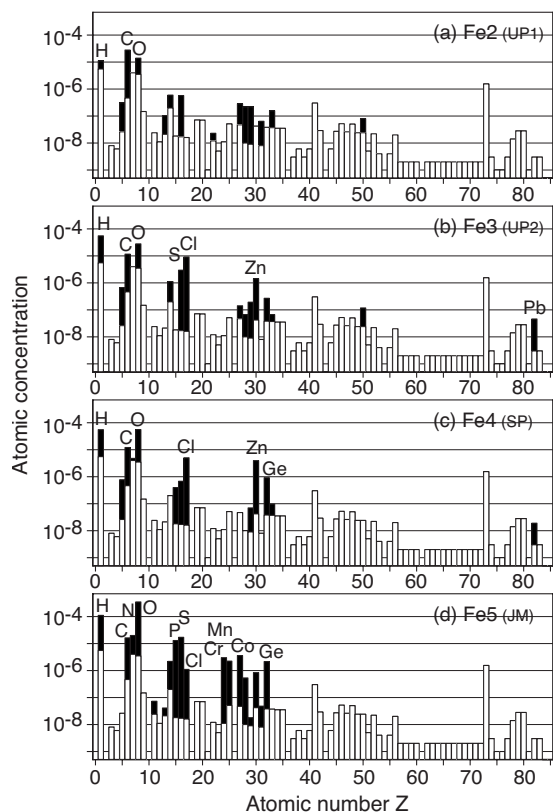
FIG. 1. Results of impurity analysis of Fe2–Fe5. Amounts of C and O were analyzed by the infrared absorption method, those of H and N by the thermal conductivity method, and those of the rest of the elements by GDMS. All results are given as mass ppm and were simply converted into atomic concentration in the figure. The shaded bars indicate that meaningful values were detected for impurity concentration greater than the lower detection limit (shown by the white bars). The sum of the amounts of impurities at the detection limit is 17 appm. The detection limit for Ta ($Z=73$) is higher (1.5 appm) because the specimen stage of the GDMS system contains Ta.

impurities were 60, 115, 140, and 540 appm for Fe2, Fe3, Fe4, and Fe5, respectively. The major impurities were carbon and oxygen for Fe2. Note that a considerable amount of substitutional impurities is present in low-purity specimens. Fe1 was a high-purity specimen processed by zone refining in a high vacuum and annealing in wet and dry hydrogen atmosphere, as described in Ref. 20. The residual resistivity ratio of Fe1 was about 3000, but the detailed impurity of this specimen could not be analyzed because of the small amount of specimen available.

Specimens for high-voltage electron microscopy (HVEM) were prepared as follows. Disc specimens of 3 mm diameter were punched from a 0.06-mm-thick ribbon-shaped Fe1 sheet. Thin foil specimens Fe1 for electron microscopy were prepared by electropolishing in two steps: twin-jet polishing and final polishing in $HClO_4$:C_2H_5OH (1:19) solution. Block specimens of Fe2–Fe5 were cold rolled to 0.1 mm thickness, and then disk specimens of 3 mm diameter were punched from the resulting sheet. The surface layer of each specimen was chemically etched in H_2O_2:HF:H_2O (50:3:6)
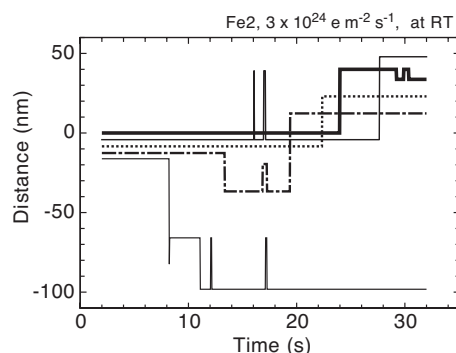

FIG. 2. Typical examples of trajectory of interstitial clusters in Fe2 under irradiation with 1250 kV electrons at room temperature; the irradiation intensity was 3×10^{24} e/m^2 s. The position of each cluster is measured along the direction of 1D migration.

solution followed by rinsing in H_2O_2:H_2O (1:1). Then, each disk specimen was wrapped in molybdenum foil and annealed in a quartz glass tube for 4 h at 1098 K in a vacuum of about 10^{-4} Pa. Then, the TEM specimens of Fe2–Fe5 were prepared by electropolishing as described above.

Electron irradiation and *in situ* observation were performed with a JEMARM-1250 high-voltage electron microscope at Tohoku University, operating at an acceleration voltage of 1250 kV. The irradiation temperature was room temperature, and the electron current density range was 1 $\times 10^{24}$–15×10^{24} e m^{-2} s^{-1}, which corresponds to a damage rate range of about 0.007–0.1 dpa s^{-1}, applying 20 eV for the threshold energy for atomic displacement (E_d). All irradiations and observations were performed using bright field images along the direction between $\langle 111 \rangle$ and $\langle 100 \rangle$ by exciting 011 systematic reflections. Images on the fluorescent screen were recorded on a video recorder through a charge coupled device camera at a frame rate of 1/30 s. The recorded area was 334×171 or 445×228 nm^2 at magnification factors of 8×10^4 and 6×10^4, respectively. The behavior of individual defect clusters was analyzed frame by frame after irradiation. The smaller limit of interstitial clusters observed was around 3 nm in the present experimental condition.

III. EXPERIMENTAL RESULTS

A. One-dimensional migration observed under electron irradiation

In the standard experiments, each area was irradiated for several minutes at a beam intensity of 3×10^{24} e m^{-2} s^{-1} (i.e., 0.02 dpa s^{-1}). The number of observed interstitial-type defect clusters increased within a few tens of seconds after the start of irradiation. Nucleated interstitial clusters grew larger and simultaneously caused 1D migration. Figure 2 shows several examples of positional changes of interstitial clusters in Fe2 measured along the direction of 1D migration under electron irradiation. Most of 1D migrations appeared as discrete jumps (namely, stepwise positional changes) at irregular intervals, and the frame-by-frame analysis (time resolution of 1/30 s) detected no details of 1D migration

trajectory at the present irradiation temperature. In addition to isolated jumps, sets of several successive jumps were frequently observed. Sometimes these jumps appeared to be back and forth motions between certain points, as shown in Fig. 2. Over 85% of 1D jumps observed in the five specimens were approximately along the projection of $\langle 111 \rangle$ and the rest were of $\langle 100 \rangle$, which is consistent with previous reports.[13,14,21] On the other hand, according to the Burgers vector examination using $\mathbf{g} \cdot \mathbf{b} = 0$ criteria with a conventional 200 kV TEM; among 80 clusters observed in Fe2 specimen after electron irradiation for 60 s, 24 and 26 clusters were identified as $1/2\langle 111 \rangle$ and $\langle 100 \rangle$, respectively. It is considered that clusters of $1/2\langle 111 \rangle$ type have a larger probability to cause 1D jumps.

In addition to 1D jumps at certain distances, some clusters suddenly appeared or disappeared. Several processes are thought to be responsible for the sudden appearance. The first is a 1D jump into the recorded area from outside the recorded area. Such a case is inevitable near the periphery of the recorded area, although the recorded area was larger than the typical jump distance. The second is that clusters hidden by a geometrical overlap with other clusters cause the 1D jump to a place where they can be observed. The third is the change in the Burgers vector of interstitial clusters under observation[21] from an invisible condition with TEM (i.e., $\mathbf{g} \cdot \mathbf{b} = 0$) to a visible condition. These three processes were not distinguished from one another in the present experimental analysis. For the sudden disappearance of interstitial clusters, a fourth process is possible, that is, the 1D migration or growth of interstitial clusters, where the clusters reached the specimen surface and disappeared. The sudden appearance and disappearance of interstitial clusters were counted as a single 1D jump event in the present analysis. The total fraction of these events was less than 25% of all the events observed.

B. Distribution of one-dimensional jump distance

The projected distance of each 1D jump was measured and converted into jump distance, assuming that the 1D jump direction was $\langle 111 \rangle$ or $\langle 100 \rangle$. Figure 3 shows the distribution of 1D jump distances observed from the start of the irradiation up to 240 s later. A common tendency observed was that the occurrence of 1D jumps monotonically decreases with increasing 1D jump distance. In the high-purity specimens, e.g., Fe1 and Fe2, the jump distance had a wider distribution extending up to over 100 nm. On the other hand, the jump distance hardly exceeded 30 nm in the low-purity specimens. These results clearly show that a 1D jump with a longer distance is suppressed in low-purity iron specimens. Similar results have been reported for vanadium.[15]

C. Irradiation intensity dependence

Jump frequency was defined as the average number of jumps observed per interstitial cluster per unit time. Figure 4 shows the irradiation intensity dependence of 1D jump frequency. In Fe1–Fe4, the jump frequency was higher in the early stage of irradiation and tended to slightly decrease with irradiation time. The frequency shown in Fig. 4 is the maxi-
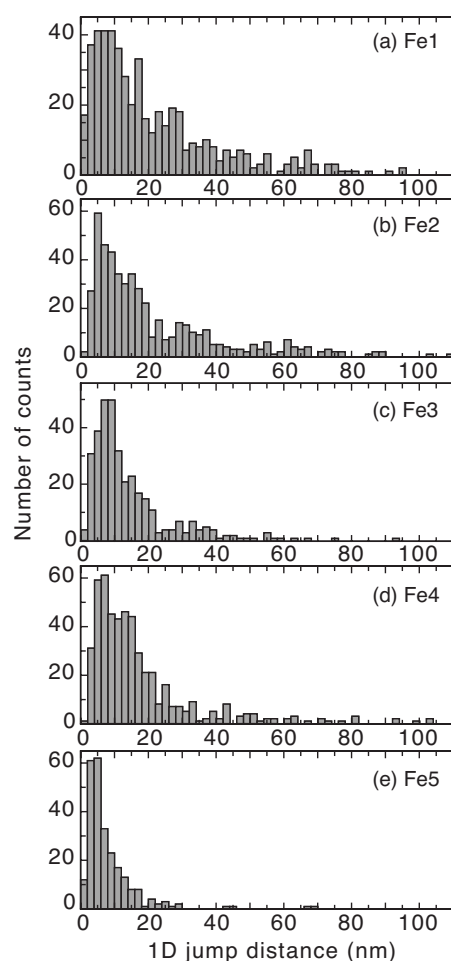

FIG. 3. Distribution of 1D jump distances observed in five iron specimens under irradiation with 1250 kV electrons at room temperature; the irradiation intensities were 3×10^{24} e/m^2 s for Fe1–Fe4 and 15×10^{24} e/m^2 s for Fe5. Data were taken at the initial 240 s of irradiation for Fe1–Fe4 and at the initial 150 s for Fe5.

mum frequency in the early stage of irradiation. In Fe5, on the other hand, the jump frequency was almost constant during the initial 120 s, and its average was plotted in Fig. 4. 1D jump frequency clearly showed positive irradiation intensity dependence for all specimens: typically, 1D jump frequency was almost proportional to beam intensity. The high-purity specimens tended to have higher jump frequency. Note that the absolute value of 1D jump frequency was close to that of the rate of atomic displacement (i.e., dpa rate) except for the low-purity specimen Fe5.

Another important observation was the rare occurrence of 1D jumps when interstitial clusters induced by HVEM irradiation were observed with conventional 200 kV TEM at room temperature. Typical cases showed that very few interstitial clusters continued to make quick back and forth motion within certain limited ranges, whereas the rest of the clusters showed no 1D migration. On the other hand, under irradiation with 1250 kV electrons, almost all the interstitial clusters seemed to make 1D jumps at random. Accordingly, electron irradiation had a significant effect of inducing interstitial clusters to make 1D jumps at approximately room temperature.
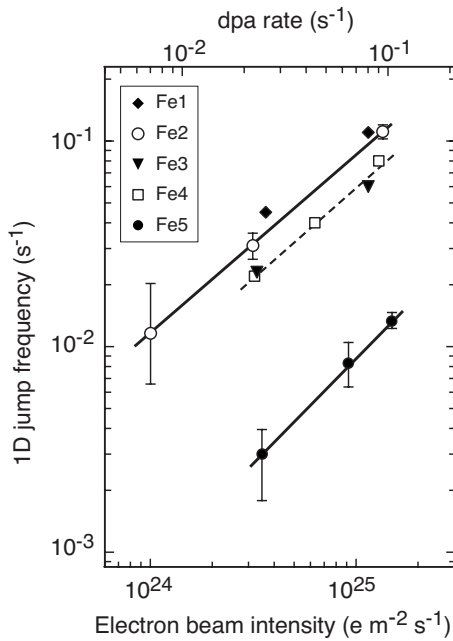
FIG. 4. Irradiation intensity dependence of 1D jump frequency for iron specimens under irradiation with 1250 kV electrons at room temperature. The dpa rate of the host iron atoms is shown on the horizontal axis.

IV. MODEL CALCULATION

To interpret the experimental results, we performed a simple model calculation of the interaction between a small interstitial cluster (7i) and a solute atom, based on molecular statics (MS) and MD methods. We selected copper as the solute atom because the interatomic potential function for Fe-Cu system was given by Ackland *et al.*[22] By analogy, we consider the effects of other impurity elements including interstitial impurities that are the major components of the present specimens. By using the Fe-Cu potential function, the average diffusion parameters have been reported for interstitial clusters (up to 20i) in Fe-1 at. % Cu.[23] Arokiam *et al.*[24,25] reported a systematic study of interaction of a small interstitial cluster in iron with a single copper atom or copper-rich precipitate.

The present calculation cell contained 3.84×10^5 mobile atoms and had fixed dimensions, as shown in Fig. 5(a). The periodic boundary condition was applied for all faces of the calculation cell. An interstitial cluster (7i) was introduced at the center of the calculation cell. Several MD simulations have shown that such a small interstitial cluster causes fast 1D migration as a crowdion bundle.[5–8] Figure 5(b) shows the cross-sectional configuration of the interstitial cluster observed along the crowdion axis. The distance r denotes the radial distance from the central axis of the crowdion bundle and the distance x denotes that along the crowdion axis.

A. Molecular statics calculation of interaction between crowdion bundle and solute copper

First, the interstitial cluster (7i) was fully relaxed using MS calculation. Figure 5(c) shows the interatomic distances
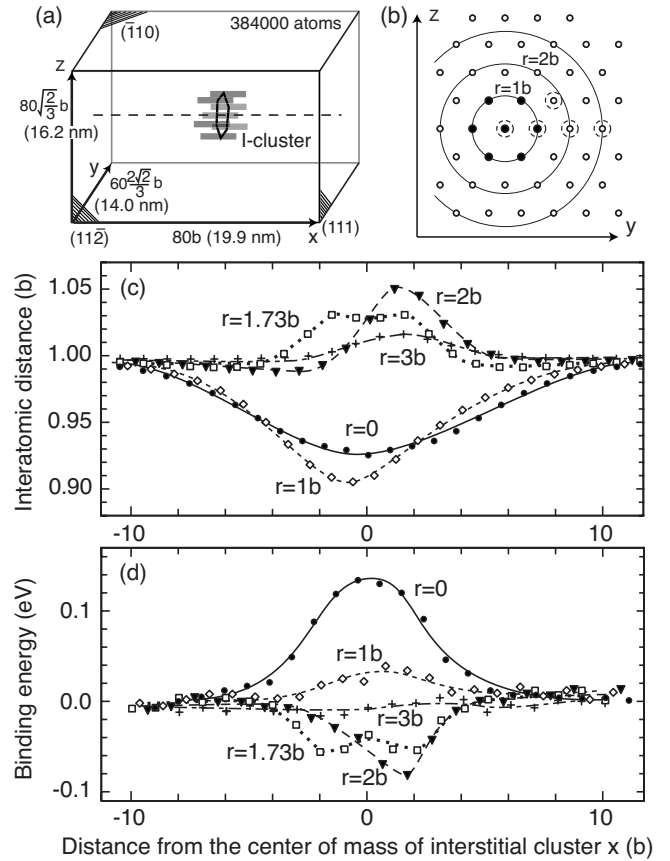

FIG. 5. (a) Schematic illustration of calculation cell used in the present molecular statics and molecular dynamics simulations. (b) Configuration of the crowdion bundle (7i) observed along the crowdion axis (x direction). The closed and open circles correspond to atomic rows with and without a crowdion, respectively. (c) Interatomic distance between neighboring atoms measured along the crowdion axis (x direction). The rows of atoms examined are shown by broken circles in (b). (d) Binding energy between the interstitial cluster (7i) and a solute copper atom located at positions shown in (c).

measured along the crowdion axis $\langle 111 \rangle$ at various positions around the crowdion bundle (7i). Inside the crowdion bundle at $r=0$ and $r=1b$ (where b denotes the atomic distance), the structure is compressional around the core of the crowdion bundle: the interatomic distance is reduced to less than 95% of the normal distance, which extends for about $8b$ along the crowdion axis. Outside the crowdion bundle at $r>1b$, the structure is dilatational around the crowdion core, and the dilatational strain decreases with increasing radial distance.

Next, an iron atom around the crowdion bundle was replaced by an oversized copper atom, and the binding energy was estimated from the difference in the total formation energy of the calculation cell after relaxation. Figure 5(d) shows the result of the calculation. As is expected from the interatomic distance, the interaction is repulsive when the copper atom is incorporated inside the crowdion bundle ($r=0$ and $r=1b$), whereas the interaction is attractive when the copper atom is incorporated outside the crowdion bundle ($r>1b$). The maximum energy of interaction was about
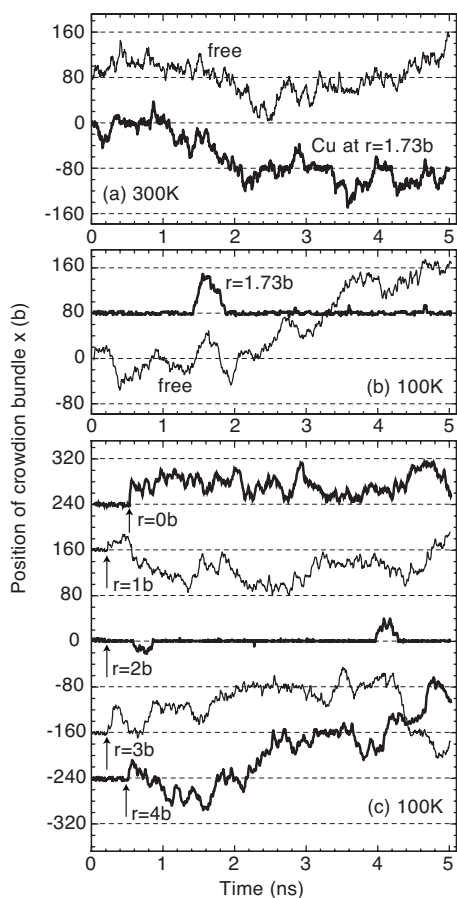
FIG. 6. Comparison of trajectory of the center of mass of the interstitial cluster (7i) with or without a solute copper atom located at $r=1.73b$ at (a) 300 K and (b) 100 K. (c) Effect of solute copper atoms at various positions on the 1D migration of the interstitial cluster (7i) at 100 K. The broken lines show the position of solute copper atoms. Arrows show the time when each solute copper atom was moved from $r=1.73b$ to the indicated position.

0.1 eV for both attractive and repulsive interactions, as reported by Arokiam *et al.* [24,25] The small interaction is thought to come from the small atomic size factor of the solute copper atom in the iron matrix, which is about 8% in this potential function.[22]

B. Molecular dynamics calculation of interaction between crowdion bundle and solute copper

The thermal migration of the crowdion bundle (7i) was examined using MD calculation. The thin lines in Figs. 6(a) and 6(b) show the migration of the center of mass of the crowdion bundle at 300 and 100 K, respectively. In the present MD calculation up to 5 ns, the migration was purely one-dimensional and involved no rotation of the crowdion axis or configurational change due to pipe diffusion. One jump was considered to occur when the center of mass of the crowdion bundle moved by one atomic distance. Then the jump frequency and the correlation factor of the crowdion bundle (7i) were determined to be 8×10^{11} jumps/s and 4.5,

respectively, at 300 K. These results are consistent with published results.[5–8]

The thick lines in Figs. 6(a) and 6(b) show the migration of the center of mass of the crowdion bundle after an iron atom outside the crowdion bundle ($r=1.73b$) was replaced by a copper atom. The migration of the crowdion bundle was almost suppressed at 100 K due to trapping: the crowdion bundle was within a few atomic distances from the copper atom (located at $x=80$ in Fig. 6(b)), except that free 1D migration took place for 0.5 ns from detrapping to another trapping. Figure 6(a) shows that the effect of trapping is less evident under the same geometrical condition at 300 K. These results are understood by considering thermal energy with respect to the binding energy between the crowdion bundle and the oversized copper atom.

Figure 6(c) shows the migration of the crowdion bundle (7i) at 100 K with a copper atom located at various radial distances from the central axis. When a copper atom is on the central axis ($r=0$), the crowdion bundle cannot overcome the copper atom due to repulsive interaction. Instead, the cluster causes short-range 1D migration between two copper atoms because the periodic boundary condition corresponds to a periodic array of copper atoms with a mutual distance of $80b$. For $r=1b$, the repulsive interaction seems to be weaker than that for $r=0$ because the crowdion bundle overcomes the solute atom twice during the same period. When a copper atom is outside the crowdion bundle ($r>1b$), the attractive interaction weakens with increasing radial distance from the axis and is not significant for $r=4b$. We note that the present results for $r=0$ and $r=2b$ are consistent to previously reported ones.[24,25]

C. Molecular dynamics calculation of detrapping of crowdion bundle from solute copper by electron irradiation

We examined detrapping assisted by a hit with electrons under HVEM irradiation conditions. The maximum kinetic energy transferred to iron and copper atoms by a head-on collision of 1250 kV electrons is about 100 eV. We selected a stable complex of a crowdion bundle (7i) and copper atom ($r=1.73b$) at 100 K (the configuration is shown in the inset of Fig. 7 and is denoted as 'initial') and gave a kinetic energy of 30 or 100 eV to the copper atom. About 30 trials were conducted while varying the timing, energy, and direction of knock-on atoms. Occasionally, the kinetic energy induced permanent point defects (during MD time scales) and/or changed the configuration of the crowdion bundle. Four typical cases of the configurational change and migration of the crowdion bundle are shown in Fig. 7.

(a) A kinetic energy of 100 eV was given to a copper atom along the direction toward the core of the crowdion bundle at $t=0.1$ ns. The copper atom was displaced from its original site ($r=1.73b$) and incorporated into the crowdion bundle, and simultaneously several pairs of displaced atoms and vacancies were produced. After 1.1 ps, all the vacancies produced recombined to disappear with interstitial atoms, resulting in a change in the configuration of the interstitial cluster and the incorporation of a copper atom into the cen-
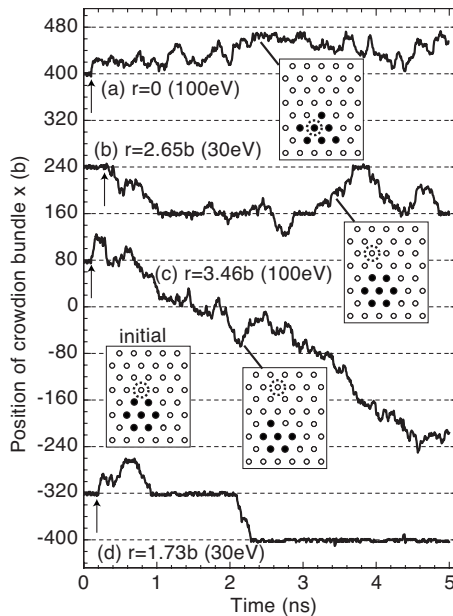
FIG. 7. Effect of a kinetic energy given to a solute copper atom on the 1D migration of the interstitial cluster (7i) initially trapped by the copper atom located at $r=1.73b$. Kinetic energy of 100 or 30 eV is given to the copper atom at the time indicated by the arrow in the figure. Inset shows the configuration of interstitial clusters observed in the x direction. The closed and open circles correspond to atomic rows with and without a crowdion, respectively. The dotted circle shows the atomic row containing the solute copper atom.

tral part of the cluster, as shown in the inset of Fig. 7. Thereafter, the crowdion bundle caused 1D migration, but did not overcome the copper atom.

(b) A kinetic energy of 30 eV was given to a copper atom along the direction toward the outside of the crowdion bundle at 0.3 ns. After the recombination of point defects, the copper atom was displaced from $r=1.73b$ to $2.65b$, while the configuration of the interstitial clusters remained unchanged. Then, the attractive interaction between the interstitial cluster and the copper atom became weaker, and detrapping occurred several times.

(c) A kinetic energy of 100 eV was given to a copper atom along the direction toward the outside of the crowdion bundle at 0.1 ns. After the recombination of point defects, the copper atom was displaced from $r=1.73b$ to $3.43b$, and a single interstitial atom was removed from the interstitial cluster. Figure 7(c) shows the center of mass of the remaining part of the interstitial cluster (6i); the cluster is almost free from the solute copper atom. The removed interstitial atom escaped from the cluster via a combination of 1D migration and crowdion axis rotation.

(d) A kinetic energy of 30 eV was given to a copper atom at 0.2 ns. After the recombination of point defects, both the position of the copper atom and the configuration of interstitial clusters remained unchanged. The kinetic energy assisted the detrapping of the cluster from the copper atom. After free 1D migration for about 0.7 ns, the cluster was trapped again by the same copper atom.
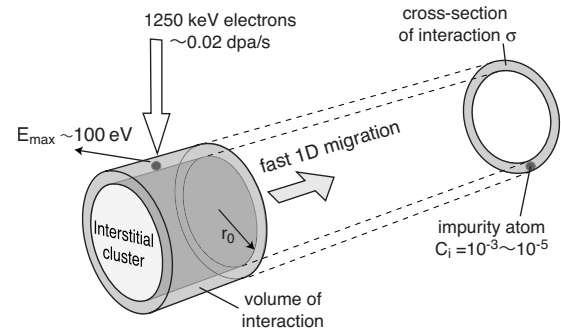

FIG. 8. Schematic illustration of the present model of 1D jumps of interstitial clusters observed under HVEM irradiation conditions.

V. DISCUSSION

A. Model of one-dimensional jumps of interstitial clusters under electron irradiation

By taking the results of MD simulations[4–8] into account, the present model assumes that interstitial clusters are highly mobile along the direction of a Burgers vector with low activation energy. Interstitial clusters in a stationary state that are usually observed with TEM are due to the trapping effect of impurity atoms, and they change into the mobile state after detrapping. When the binding energy between an impurity atom and an interstitial cluster is sufficiently large, detrapping is not thermally activated around room temperature. Instead, detrapping is assisted by electron irradiation, as has been suggested by the electron irradiation intensity dependence of 1D jump frequency (see Fig. 4). The present model considers the effects of kinetic energy transferred to atoms around the trap by the collision of incident electrons. When the transferred energy is sufficiently large, an impurity atom is displaced from its original site and travel through the crystal for a few atomic distances. When an impurity atom is far from the interstitial cluster, the cluster becomes free from the attractive interaction exerted by the impurity atom. In addition, results in Fig. 7(d) suggest that a high kinetic energy causes another detrapping without displacing the impurity atom.

An interstitial cluster that detrapped from impurity atoms is expected to cause free 1D migration until it is trapped again by another impurity atom. According to the MD simulation, the diffusivity of a free cluster 91i (about 2.5 nm in size) is approximately 2×10^{-8} m^2/s at 300 K,[8] which corresponds to a mean diffusion length of 30 μm at $1/30$ s. If this diffusivity is not an overestimate for interstitial clusters observed in the present experiments (average size of 5–8 nm), it must be difficult to observe details of fast 1D migration with TEM when the irradiation and observation are performed at room temperature. The interstitial cluster should be observed to make jumps from one impurity atom to another at irregular timings. The present model is schematically shown in Fig. 8.

Generally, interstitial clusters that have grown sufficiently large to be observed with TEM are considered not to be highly mobile essentially, and all interstitial clusters observed with TEM in a stationary state are considered not due to the effect of trapping by impurity atoms. However, inter-

stitial clusters are easily associated with impurity atoms, when one considers the heterogeneous nucleation of interstitial clusters at impurity atoms under electron irradiation. Even if interstitial clusters are nucleated without the help of impurity atoms, 1D migration will transport clusters to impurity atoms; otherwise, the clusters will reach the surface of thin foils and disappear. In addition, the concentration of interstitial clusters is around 10^{-7} under typical irradiation conditions, which is much lower than the impurity concentration even in high-purity specimens. Accordingly, it is very likely that interstitial clusters that can be observed with TEM in a stationary state are trapped by impurity atoms.

B. Analysis of distribution of one-dimensional jump distance

Based on the above model, in this section, we examine whether the experimental distribution of 1D jump distance is determined by the interaction between interstitial clusters and impurity atoms. We consider a certain volume around individual interstitial clusters and assume that a certain impurity atom in this volume prevents the free migration of an interstitial cluster due to their binding. Let the cross section of the interaction volume projected along the direction of 1D migration be σ. For convenience, the cross-section is expressed in numbers of atoms contained in the region. We assume a random distribution of impurity atoms at the concentration $C_i (\ll 1)$ and neglect the migration of impurity atoms during the fast 1D migration of interstitial clusters for simplicity. When an interstitial cluster migrates for one atomic distance along the direction of a Burgers vector, its interaction volume is assumed to be translated without changing its shape. Then the interaction volume absorbs one or no impurity atoms with the probabilities σC_i and $(1 - \sigma C_i)$, respectively. Accordingly, a 1D jump of length n, namely, an interstitial cluster detrapped from an impurity atom and trapped again by another impurity atom after 1D migration for n atomic distances, is approximated to have a probability of

$$P(n) = (1 - \sigma C_i)^{n-1} \sigma C_i. \qquad (1)$$

This simple model suggests an exponential decrease in the occurrence of 1D jumps with increasing jump distance. By taking the logarithm of both sides of Eq. (1), we obtain

$$\ln P(n) = (n - 1)\ln(1 - \sigma C_i) + \ln \sigma C_i. \qquad (1')$$

The distribution of 1D jump distance shown in Fig. 3 is replotted in Fig. 9 using a logarithmic scale for the number of 1D jumps. When we neglect the region of jump distances less than 10 nm for experimental difficulties and also that of long distances for poor statistics, the middle range for each specimen is well described by a straight line. The gradient of the line corresponds to $\ln(1 - \sigma C_i)$ and is nearly equal to $-\sigma C_i$ for $\sigma C_i \ll 1$. The σC_i values obtained from the gradient of the line were greater for the low-purity specimens, as shown in Table I. By using the average size of interstitial clusters that caused 1D jumps, the numbers of atoms on the plane (S) and the line dislocation (L) were obtained assuming circular shape. By assuming these values to be the cross section σ of the interaction volume projected along the di-
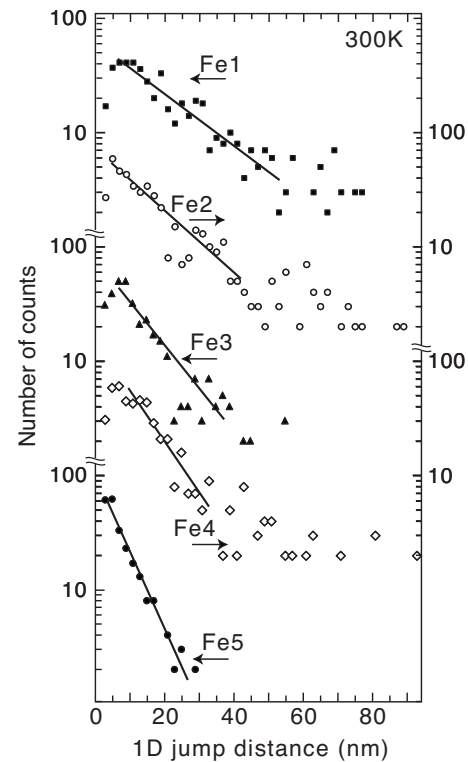

FIG. 9. Semi-logarithmic plot of the distribution of the 1D jump distance shown in Fig. 3.

rection of 1D migration, the concentration of impurities that contributed to trapping was estimated and plotted in Fig. 10 with the results of impurity analysis. The concentration C_i roughly corresponds to the total number of impurity atoms obtained by impurity analysis, when one takes the line dislocation with a width of two or three atomic distances as the cross section of the interaction volume ($\sigma = 2L$ or $\sigma = 3L$). Because this cross section is thought to be a reasonable value, we infer that most of the impurity atoms detected by the analysis contribute to the trapping of interstitial clusters. Note that the contribution of hydrogen can be neglected because hydrogen has a large diffusivity and a small solubility that result in its segregation into grain boundaries or dislocations prior to the irradiation.

C. Interaction between interstitial cluster and solute element

In the simple model presented above, we considered only attractive interactions between an impurity atom and an interstitial cluster through a certain threshold-type volume that causes trapping. Practical elastic interaction is expected to depend on several parameters as discussed below.

A small interstitial cluster is regarded as a crowdion bundle of cylindrical shape (radius r_0), as shown in Fig. 8. Compressional strain along the crowdion axis presents inside the crowdion bundle ($r < r_0$), whereas dilatational strain presents outside the crowdion bundle ($r > r_0$). The above simulations for the Fe-Cu system suggest that oversized copper atoms are unstable inside the crowdion bundle and act as a barrier for 1D migration. On the other hand, oversized cop-

TABLE I. Parameters used to estimate the cross section of interaction between interstitial clusters and impurity atoms, and results of impurity analysis shown in Fig. 1. The values related to the cross section are shown in numbers of atoms.

	Fe1	Fe2	Fe3	Fe4	Fe5
σC_i (atoms)	0.013	0.016	0.022	0.025	0.039
Average size of interstitial clusters (nm)	7.9	7.2	7.8	7.8	5.1
Length of loop dislocation L (atoms)	100	91	100	100	65
Area of dislocation loop S (atoms)	800	660	780	780	330
Total concentration of C, O, and N (appm)		46	44	73	390
Total concentration of impurities except H (appm)		49	60	85	430

per atoms are stable outside the cylindrical surface of the crowdion bundle to serve as a trap of the crowdion bundle. The magnitude of the interaction decreases with increasing radial distance of the solute atom.

The situation is expected to be reversed for undersized solute atoms; the crowdion bundle is trapped by undersized solute atoms inside the crowdion bundle ($r < r_0$), and undersized solute atoms are unstable outside the crowdion bundle ($r > r_0$). Interstitial impurities are expected to have similar effects to oversized atoms. Accordingly, all impurities may serve as both a barrier and a trap for crowdion bundles depending on their atomic size and mutual geometry. A large interstitial cluster, which is well described as an interstitial-type dislocation loop, is thought to interact with solute atoms similar to the crowdion bundle described above, except that strong interaction is restricted to the vicinity of the loop dislocation instead of the whole cylindrical body.

The interaction energy is larger for substitutional impurity atoms with a larger difference in atomic size. Moreover, interstitial impurity atoms are expected to have a strong interaction with interstitial clusters, as determined by MS simulation of the interaction between an interstitial carbon atom and an interstitial cluster (9i or 16i) in iron which showed a binding energy greater than 1 eV.[26]

The effect of impurity atoms on the 1D migration discussed above are expected to be common to both types of interstitial clusters, $\mathbf{b} = 1/2\langle 111 \rangle$ and $\langle 100 \rangle$. However, the magnitude of the elastic interaction between impurity atom and interstitial cluster will be larger for the latter because of the larger magnitude of the Burgers vector, which correspond to larger interaction volume and may be responsible for the low probability to cause the 1D migration.

In the above analysis, a certain threshold-type volume for trapping may be an oversimplification. The detailed 1D jump behavior cannot always be explained by this simple model. In the back and forth motions of interstitial clusters, for example, successive 1D jumps, take place at short intervals between certain points, as shown in Fig. 2, while the average jump interval is about 30 s under the irradiation condition. This would be the effect of the weak binding between interstitial clusters and impurity atoms, probably due to the smaller difference in atomic size or longer mutual distance. Note that repulsive interactions will not markedly affect the process mentioned above because the free migration of interstitial clusters associated with pure repulsive interaction will not induce the formation of interstitial clusters in a stationary state.

D. One-dimensional jump frequency under electron irradiation

In the present model, 1D jump frequency corresponds to the detrapping rate of interstitial clusters from impurity atoms. We proposed above that detrapping may be mainly caused by the displacement of impurity atoms due to being hit by electrons. The simplest case involves a single impurity atom operating as a trap per interstitial cluster and being removed from the interaction volume by a single hit by an electron. If this is the case, 1D jump frequency should be directly proportional to electron beam intensity through the rate of atomic displacement (i.e., dpa rate).

Experimental 1D jump frequency was almost proportional to electron beam intensity, and the absolute value of 1D jump frequency was close to that of dpa rate for Fe1-Fe4. Then, the probability of a 1D jump event occurring is comparable to the probability of the kinetic energy transfer from electrons to each host iron atom being greater than 20 eV (E_d).
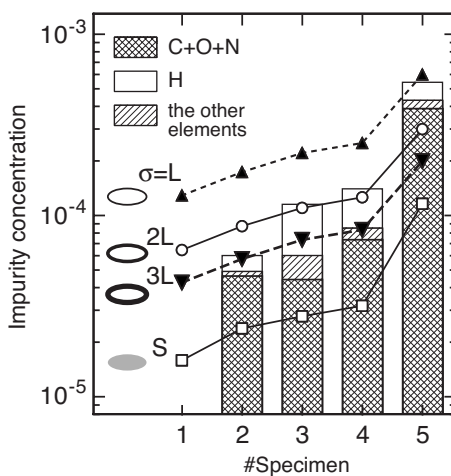

FIG. 10. Comparison of the impurity concentration of the specimens used. The bar graph summarizes the results of impurity analysis shown in Fig. 1. Points are concentrations of impurities affecting the 1D migration of interstitial clusters that were estimated from the distribution of 1D jump distance, while assuming four values as cross sections for interactions.

The detailed jump frequency, however, slightly differed depending on the purity of specimens, which could be interpreted as follows. Interstitial impurity atoms are expected to have a larger displacement rate than the host iron atom or other substitutional impurity atoms due to their small mass and probably to the small energy of binding to the crystal lattice. This will result in a large jump frequency in high-purity specimens, in which the fraction of substitutional impurity atoms is very small. On the other hand, the low-purity specimen Fe5 contains a considerable number of substitutional impurity atoms. In addition, it may be possible in this low-purity specimen that a single interstitial cluster is trapped by multiple impurity atoms.

E. Brief comments

The experimental results and analysis suggest that the intrinsic 1D migration of interstitial clusters is markedly affected by trace impurity elements even in high-purity specimens. The proposed model explains the experimental 1D migration behavior under electron irradiation, without qualitatively contradicting recent results of MD simulations that predict fast 1D migration.

An atomistic simulation has suggested that vacancies are possible to reduce the 1D migration of interstitial clusters.[27] Vacancies are considered to be highly mobile in high-purity iron at room temperature,[28] and to have a concentration around 10^{-4} under a steady-state of electron irradiation at a damage rate of 10^{-2} dpa s^{-1}, according to a simple reaction rate analysis.[29] The vacancy concentration is comparable to the impurity concentration in the present experimental condition. However, our recent result of the 1D jump distribution in Fe1 under a high damage rate (0.08 dpa s^{-1}) almost corresponds to that at 0.02 dpa s^{-1} shown above, though the steady-state concentration of vacancies are expected to increase in proportion to the square root of the damage rate.[29] It is considered that a contribution of the vacancies is negligible in the present experimental condition.

It is not yet clear whether impurities also have a similar effect on interstitial clusters under the condition without electron irradiation. Generally, the 1D migration of interstitial clusters is a rare event during postirradiation observations of neutron- and ion-irradiated specimens with conventional 200 kV TEM, as well as during the observation after electron irradiation presented in Sec. III C. It is natural to consider that stationary interstitial clusters are also "trapped" by impurity atoms or solute atoms at room temperature. If this is the case, the 1D migration observed with 200 kV TEM at low probabilities is caused by detrapping from impurities with relatively weak binding. The possible trigger of such detrapping may be thermal activation, local stresses, and also irradiation with 200 kV electrons for light interstitial impurity atoms depending on the material and conditions. At elevated temperatures, interstitial clusters have been reported to cause 1D migration with dragging interstitial impurities.[14]

Finally, we note an importance of a possible effect of substitutional solute atoms at high concentration[30] as well as that of trace interstitial impurity atoms for modeling the 1D migration of interstitial clusters in practical alloys.

VI. CONCLUSION

We examined experimental 1D jumps of interstitial clusters in iron having different purities under electron irradiation at room temperature. We interpreted the 1D jump to proceed as follows: (1) stationary interstitial clusters are trapped by impurity atoms through attractive interactions, (2) incident electrons hit and displace impurity atoms to cause detrapping, (3) free clusters cause fast 1D migration at low activation energy, and (4) free clusters are trapped again by other impurities. The experimental distributions of 1D jump distance and 1D jump frequency are successfully explained by the model. In molecular dynamics simulation, we demonstrated the trapping of interstitial clusters (7i) by an oversized solute copper atom, the detrapping assisted by the kinetic energy given to the copper atom, and the subsequent free 1D migration of interstitial clusters until another trapping.

[1] A. I. J. Foreman, W. J. Phythian, and C. A. English, Philos. Mag. A **66**, 671 (1992).

[2] A. F. Calder and D. J. Bacon, J. Nucl. Mater. **207**, 25 (1993).

[3] W. J. Phythian, R. E. Stoller, A. E. J. Foreman, A. E. Calder, and D. J. Bacon, J. Nucl. Mater. **223**, 245 (1995).

[4] B. D. Wirth, G. R. Odette, D. Maroudas, and G. E. Lucas, J. Nucl. Mater. **244**, 185 (1997).

[5] N. Soneda and T. Diaz de la Rubia, Philos. Mag. A **78**, 995 (1998).

[6] N. Soneda and T. Diaz de la Rubia, Philos. Mag. A **81**, 331 (2001).

[7] Yu. N. Osetskey, D. J. Bacon, A. Serra, B. N. Singh, and S. I. Golubov, J. Nucl. Mater. **276**, 65 (2000).

[8] Yu. N. Osetskey, D. J. Bacon, A. Serra, B. N. Singh, and S. I. Golubov, Philos. Mag. **83**, 61 (2003).

[9] C. H. Woo and B. N. Singh, Philos. Mag. A **65**, 889 (1992).

[10] H. Trinkaus, B. N. Singh, and A. J. E. Foreman, J. Nucl. Mater. **199**, 1 (1992).

[11] H. Trinkaus, B. N. Singh, and A. J. E. Foreman, J. Nucl. Mater. **249**, 91 (1997).

[12] H. L. Heinisch and B. N. Singh, Philos. Mag. **83**, 3661 (2003).

[13] M. Kiritani, J. Nucl. Mater. **206**, 156 (1993).

[14] M. Kiritani, J. Nucl. Mater. **251**, 237 (1997).

[15] T. Hayashi, K. Fukumoto, and H. Matsui, J. Nucl. Mater. **307-311**, 993 (2002).

[16] K. Arakawa, M. Hatanaka, H. Mori, and K. Ono, J. Nucl. Mater. **329-333**, 1194 (2004).

[17] H. Abe, N. Sekimura, and Y. Yang, J. Nucl. Mater. **323**, 220 (2003).

[18] K. Arakawa, K. Ono, M. Isshiki, K. Mimura, M. Uchikoshi, and H. Mori, Science **318**, 956 (2007).

[19] Y. Matsukawa and S. J. Zinkle, Science **318**, 959 (2007).

[20] S. Takaki and H. Kimura, Scr. Metall. **10**, 1095 (1976).

[21] K. Arakawa, M. Hatanaka, E. Kuramoto, K. Ono, and H. Mori, Phys. Rev. Lett. **96**, 125506 (2006).

[22] G. J. Ackland, D. J. Bacon, A. F. Calder, and T. Harry, Philos. Mag. A **75**, 713 (1997).

[23] J. Marian, B. D. Wirth, A. Caro, B. Sadigh, G. R. Odette, J. M. Perlado, and T. Diaz de la Rubia, Phys. Rev. B **65**, 144102 (2002).

[24] A. C. Arokiam, A. V. Barashev, D. J. Bacon, and Y. N. Osetsky, Philos. Mag. Lett. **85**, 491 (2005).

[25] A. C. Arokiam, A. V. Barashev, D. J. Bacon, and Y. N. Osetsky, Philos. Mag. **87**, 925 (2007).

[26] K. Tapasa, A. V. Barashev, D. J. Bacon, and Yu. N. Osetsky, J. Nucl. Mater. **361**, 52 (2007).

[27] M. Pelfort, Yu. N. Osetsky, and A. Serra, Philos. Mag. Lett. **81**, 803 (2001).

[28] S. Takaki, J. Fuss, H. Kugler, U. Dedek, and H. Schultz, Radiat. Eff. **79**, 87 (1983).

[29] M. Kiritani, N. Yoshida, H. Takata, and Y. Maehara, J. Phys. Soc. Jpn. **38**, 1677 (1975).

[30] G. A. Cottrell, S. L. Dudarev, and R. A. Forrest, J. Nucl. Mater. **325**, 195 (2004).